NASA TECHNICAL MEMORANDUM

NASA TM X-71656

NASA TM X-71656

FORWARD VELOCITY EFFECTS ON UNDER-THE-WING EXTERNALLY BLOWN FLAP NOISE

by J. Goodykoontz, U. von Glahn,
and R. Dorsch
Lewis Research Center
Cleveland, Ohio 44135

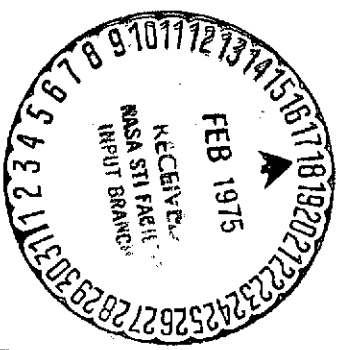

TECHNICAL PAPER to be presented at
Second Aero-Acoustics Specialists Conference
sponsored by the American Institute of Aeronautics
and Astronautics
Hampton, Virginia, March 24-26, 1975

FORWARD VELOCITY EFFECTS ON UNDER-THE-WING EXTERNALLY BLOWN FLAP NOISE

J. Goodykoontz,* U. von Glahn,** and R. Dorsch†

National Aeronautics and Space Administration
Lewis Research Center
Cleveland, Ohio 44135

Abstract

Noise tests were conducted with small-scale models of externally blown-flap powered-lift systems that were subjected to simulated takeoff and landing free-stream velocities by placing the nozzle-wing models in a free jet. The nozzle configurations consisted of a conical and an 8-tube mixer nozzle. The results showed that the free-stream velocity attenuated the noise from the various configurations, with the amount of attenuation depending on the flap setting. More attenuation was obtained with a flap setting of 20° than with a flap setting of 60°. The dynamic effect on the total attenuation caused by aircraft motion is also discussed.

Introduction

A number of experimental model studies have been made in order to determine the noise generating characteristics of short-haul aircraft employing an externally blown flap (EBF) powered-lift system with lower surface blowing (refs. 1 to 6). The results have shown that flap noise is proportional to the sixth power of the peak jet impingement velocity at the flap location. Thus, a small increase in the jet impingement velocity due to any cause can result in a substantial rise in flap noise.

Experimental work on the effect of forward velocity on jet flows (ref. 7) has shown that with forward velocity the jet flow field is stretched axially so that at a given point downstream of the nozzle exhaust plane (such as the flap location) the local velocities are increased. This implies that an increase in flap noise should be incurred with forward velocity compared to that obtained statically. At the same time, however, forward speed alters the flow field about the wing-flap system which has an undetermined acoustic effect. Furthermore, the jet exhaust noise is attenuated by the free-stream velocity. The net effect of forward velocity on the noise signature of an EBF system under the preceding simultaneous complex effects is presently not well understood.

Very limited acoustic data (ref. 8) obtained with a large-scale EBF model in a wind tunnel showed that the free stream velocity, herein also called relative velocity effect, decreased the noise level only about 2 dB in the low frequency range when the flaps were highly deflected as would be the case for landing (forward velocity about 45 m/sec).

The purpose of this report is to present the results of an experimental program that was undertaken at the NASA Lewis Research Center to investigate the acoustic characteristics of a model EBF system when exposed to a free-stream velocity in a free jet. Comparisons are made between the data obtained statically (without airspeed) and that obtained with airspeed to show the magnitude of the effect of forward airspeed on various model EBF configurations. The configurations included a conical nozzle (5.08 cm diameter), an 8-tube mixer nozzle (3.98 cm equivalent diameter), and a model wing (32.4 cm chord) with two trailing flaps that could be placed at various settings relative to the wing chordline. Forward airspeed was simulated by flow from a free jet (nozzle diameter, 33 cm). The test nozzles and model wing were mounted downstream of the exhaust plane of the free jet and centered on its axis. Nominal jet exhaust velocities ranged from 208 to 290 m/sec and free-stream velocities from zero to 53 m/sec.

Nozzle-wing configuration noise characteristics in the program are presented in terms of overall sound pressure levels (OASPL) and sound pressure level (SPL) spectra. The effect of relative motion of the noise source with respect to the observer is not accounted for in the measured acoustic data from free jets and wind tunnels. This dynamic effect is discussed herein and an approximation of this effect is calculated and shown for representative acoustic data obtained with the free jet.

Apparatus and Procedure

Facility

A 33-cm diameter free jet, described in reference 9, was used to obtain airspeed effects for the acoustic tests. Free jet velocities of 0, 43, and 53 m/sec were used in the present studies. A photograph of a typical nozzle-wing configuration installed in the free jet is shown in figure 1.

The noise data were measured by fifteen 1.27 cm diameter condenser microphones placed at various intervals on a 3.05 meters radius circle around the wing-nozzle setup. The center of the microphone circle was located at the exit of the 5.08 cm diameter convergent nozzle. The microphone circle was in a horizontal plane 3.91 meters above an asphalt surface and perpendicular to the vertically mounted wing. The plane of the microphone circle passed through the nozzle axes. A standard piston calibrator (124 ± 0.2 dB, 250 Hz tone) was used to calibrate the condenser microphones. Wind screens were placed on all microphones. The noise data were analyzed by a one-third octave band spectrum analyzer referenced to 2×10^{-5} newtons per square meter.

Strain-gage pressure transducers were used to measure total pressures upstream of the nozzles. Temperatures were measured upstream of the nozzles by thermocouples immersed in the flow stream.

Weather data were also monitored and recorded (barometer, temperature, humidity, wind speed and direction).

*Aerospace Research Engineer
**Member AIAA Chief, Jet Acoustics Branch
†Member AIAA Head, Section B, Jet Acoustics Branch

Test Models

Two different nozzles were used in this program; a 5.08 cm diameter conical nozzle and an 8-tube mixer nozzle with an equivalent diameter of 3.98 cm. The dimensions of the test setup using the 5.08 cm nozzle are shown in figure 2. The nozzle was attached to a 10.16 cm outside diameter supply line that was concentric with a 33 cm diameter convergent nozzle (fig. 2(a)). The exit of the 5.08 cm nozzle was 22.8 cm downstream of the exit of the larger nozzle. The partial span wing section is the same as that used in reference 2. The wing had two flaps that were placed in the following settings, (1) 10° - 20° (takeoff) with respect to the wing chord line, and (2) 30° - 60° (landing). The wing had a partial span of 61 cm and a chord length of 32.4 cm with the flaps retracted. The leading edge of the wing was set at 6.06 cm downstream of the exit of the 5.08 cm nozzle and 9.15 cm from the nozzle axis. The wing chord line was at a 5 degree angle of attack relative to the nozzle axis. The wing was mounted with the spanwise direction in a vertical plane. Details of the conical nozzle are shown in figure 2(b).

In figure 3(a) the dimensions and arrangement of the 8 tube mixer nozzle of the wing setup are shown. The 8 tube nozzle exit was located 31.40 cm downstream of the exit of the 33 cm nozzle and 2.54 cm downstream of the leading edge of the wing. Again, the leading edge of the wing was 9.15 cm from the axis of the nozzle and the wing chord line was set at a 5 degree angle of attack relative to the nozzle axis. Figure 3(b) gives the details of the 8 tube nozzle. The nozzle had eight 1.41-cm inside diameter tubes equally spaced with centers on an 8 cm diameter circle. A conical afterbody was installed to prevent flow separation. The equivalent diameter of the 8 tube nozzle (diameter of single tube with same total exit area) was 3.98 cm.

Procedure

Far field noise data were taken in the flyover plane for various jet velocities. The test procedure was to obtain steady flow conditions for a given total pressure upstream of each nozzle. Three noise data samples were taken at each microphone location. An atmospheric loss correction was applied to the average of the three samples to give lossless sound pressure level data at 3.05 meters.

The noise from the free jet (large nozzle) contributed substantially to the total noise of the system only in the low frequency region of the spectra (below 400 Hz). Therefore, the effect of the free-stream velocity on the noise from the small nozzle-wing configurations is shown only for those frequencies for which the contribution of the free jet can be considered negligible (generally less than 1 dB).

Nozzle exhaust velocities were calculated from the isentropic equations using the total pressures and temperatures measured upstream of the nozzle exhaust planes.

Results and Discussion

The acoustic data are presented in terms of overall sound pressure levels and spectra. In general, the effect of the free-stream velocity was to attenuate the noise levels measured statically. However, the amount of attenuation decreased with increased flap deflection. In general, the data trends are discussed at the test directivity angles (measured from the nozzle inlet) most closely representing the maximum noise levels during flyover. Thus, the data at a directivity angle of 100° for a 10° - 20° flap setting represents the aircraft at takeoff. Similarly, the data at a directivity angle of 80° with a flap setting of 30° - 60° represents the aircraft for the landing attitude. Details of the acoustic levels, spectra and trends are discussed in the following sections.

Overall Sound Pressure Level

The overall sound pressure level (OASPL) directivity patterns for the test nozzles with the wing are shown in figure 4 with and without free-stream velocity. The data are presented in terms of OASPL as a function of the directivity angle, θ, for flap deflection angles of 10° - 20° and 30° - 60° for both the conical nozzle (fig. 4(a)) and the 8-tube mixer nozzle (fig. 4(b)). The data shown are for a nominal jet exhaust velocity of 290 m/sec; however, they are representative of data taken at the other jet velocities used in the study. It is apparent that the attenuation due to relative velocity is much greater with a 10° - 20° flap setting (clear symbols) than that with a 30° - 60° flap setting (solid symbols). At the higher flap setting, the attenuation due to relative velocity generally amounted to less than 2 dB over a range of directivity angles from 40° to 100°. Similar acoustic results are reported in reference 8 for large-scale model tests in a wind tunnel. Attenuation of OASPL due to relative velocity, in general, is similar at all directivity angles and dependent on flap setting for the range of conditions included herein. With a 30° - 60° flap setting, a significant reduction in OASPL was obtained at a directivity angle of 150° (not shown in figure 4); however, the noise level at this directivity angle is of no great significance in estimating the flyover noise for an aircraft due to the long path length from the noise source to the ground.

The OASPL values as a function of relative velocity, $U_j - U_o$, are shown for both nozzle-wing configurations in figure 5 for a 10° - 20° flap setting and in figure 6 for a 30° - 60° flap setting. Directivity angles of 100° and 80°, respectively are associated with these two flap settings. The effects of jet velocity and airspeed will be discussed in terms of power-law exponents, i. e., OASPL ~ 10 log $\left[U_j\left(1 - \frac{U_o}{U_j}\right)^a\right]^b$. The total effect of relative velocity, $U_j - U_o$, at a constant U_j is given by $k < \theta > = (a)(b)$. With zero forward velocity, the data indicate a nominal 7-power relation of the OASPL with the jet exhaust velocity for all configurations. With a free-stream velocity (free jet) the power relation of OASPL with the relative velocity ($k < \theta >$ exponent), however, is a function of the configuration and flap setting. With a 10° - 20° flap setting (fig. 5(a)), the OASPL for the conical-nozzle/wing had a nominal 3.5 power variation with relative velocity, whereas the mixer-nozzle/wing (fig. 5(b)) had a nominal 4.9 power variation with relative velocity. With a 30° - 60° flap setting, the OASPL for both configurations showed a nominal 1.4 power variation with relative velocity.

The variation of OASPL with relative velocity was correlated by using the relationship $U_j (1 - U_o/U_j)^a$ as shown in figures 7 and 8. Nominal values of the a-exponent are shown in the abscissa of the figure parts. The a-exponent is the ratio of the relative velocity power shown in figure 5 to the power for the static case hereinafter called b-exponent; for example, in figure 5(a), $a = K < \theta >/b = 3.5/7 = 0.5$. Good correlation of the data is evident for both nozzle-wing configurations and both flap settings. At other directivity angles, the a- and b-exponents differed somewhat depending on the nozzle used and the flap setting. A summary of the nominal values for these exponents is given in Table 1 for all nozzle-wing configurations, flap settings, and directivity angles.

Spectra

The effects of airspeed on the nozzle-wing spectra are summarized by the data shown in figures 9 to 16. Except as noted, the data shown are at the maximum noise directivity angles associated with flap settings for takeoff and landing.

Effect of forward speed. - In figures 9 and 10, the normalized nozzle-wing spectra are shown in the familiar terms of SPL-OASPL as a function of frequency for various airspeeds. The data shown are for a jet exhaust velocity of 290 m/sec and flap settings of 10° - 20° (fig. 9) and 30° - 60° (fig. 10) with corresponding directivity angles of 100° and 80°, respectively. For frequencies above 1200 Hz good correlation of the data, with and without airspeed, is achieved for all configurations. At frequencies below 600 Hz, the attenuation due to the airspeed is greater than that at the frequencies above 1200 Hz, as evidenced by the greater negative SPL-OASPL values obtained with the forward speed compared to those obtained statically. This anomaly will be discussed herein in a later section dealing with the identification of apparent noise sources. The data also imply that a Strouhal number correlation based on the jet exhaust velocity should be used rather than one based on jet relative velocity ($U_j - U_o$) since the latter would cause a lateral shift in the data shown in figures 9 and 10.

Effect of jet exhaust velocity. - The effect of changes in jet exhaust velocity on the spectra with a constant airspeed is shown in figures 11 and 12. The spectral data are plotted in terms of Strouhal number (based on the effective nozzle diameter and the jet exhaust velocity) for both nozzle-wing configurations and flap settings of 10° - 20° and 30° - 60° with corresponding directivity angles of 100° and 80°, respectively. The data show good correlation of the spectra over the entire frequency range for all configurations. Also it is evident again that the jet exhaust velocity rather than the jet relative velocity should be used for the Strouhal number.

Effect of Directivity Angle. - The spectra at various directivity angles are shown in figures 13 to 16, for both nozzle-wing configurations and flap settings of 10° - 20° and 30° - 60°. The data are shown in terms of SPL-OASPL as a function of frequency for forward speeds of zero and 55 m/sec and with a jet exhaust velocity of 290 m/sec. In general, the spectra shape is substantially independent of directivity angle.

Noise Sources

The spectral distribution of noise level (SPL) with frequency indicates, for static conditions, presence of several dominant noise sources. These noise sources are identified in the spectral plots shown in figure 17, in which the spectra for the nozzle alone is included as a reference level. First, noise contributed by the trailing edge of the second flap is indicated for a relatively narrow band of low frequencies (200 to 800 Hz in fig. 17). Secondly, turbulence generated broadband noise caused by the interaction of the turbulent jet exhaust with the flap surfaces is indicated at frequencies greater than about 800 Hz. Finally, the mixer nozzle-wing configuration shows a narrow band noise source peaking near 3500 Hz (fig. 17(a)). The source of this noise may possibly be associated with the jet flow through the region of the opening between the first and second flaps. This noise source may be peculiar to this type of nozzle-wing configuration. From the data shown in figure 17, it is apparent that, for the flap settings used, the trailing edge noise source (low frequencies) is independent of flap setting. The noise source near 3500 Hz in figure 17(a) appears to be similarly independent of flap setting. The broadband turbulence generated noise, however, is dependent on the flap setting. This source decreases in noise level with a decrease in flap setting as well as shifting the location of the peak noise to a lower frequency. At frequencies greater than 5000 Hz, the jet noise of the mixer nozzle is dominant.

Trailing edge noise. - A more detailed look at the low frequency (500 Hz) noise source (fig. 18) shows that it extends over a wide range of directivity angles. With a 10° - 20° flap setting, the noise level peaks near a directivity angle of 80°. Increasing the flap setting to 30° - 60° causes the peak noise location to shift to a directivity angle of less than 60°. Significant noise attenuation was obtained with forward speed for the nozzle-wing configurations and flap settings used herein. (This was previously noted in the discussion of figures 9 and 10). The relative velocity exponents applicable to this noise source are summarized in Table 2. It should be noted that these relative velocity power relations are considerably greater than those obtained for the OASPL values (figs. 5 and 6). While this low frequency noise may not contribute significantly to the perceived noise level of a full-scale aircraft, it is a problem with regard to structural vibrations and fatigue.

3500 Hz noise source. - The nominal bandwith of the nominal 3500 Hz noise source appears to be somewhat narrower than that of the low frequency source just discussed. The 3500 Hz source peaks near a directivity angle of 80° and decreases rapidly in SPL to both sides of this angle. For static conditions, the peak noise level varies with the 8-power of the jet exhaust velocity. With forward speed, the noise level of the source varies as the 4.8-power of the relative velocity.

Aircraft Motion Effects

As stated earlier, the following approximate relation, taken from reference 6, holds in the flyover plane for the decrease in OASPL due to airspeed effects:

$$\Delta(\mathrm{OASPL})_{RV} = 10\ k < \theta > \log \left(1 - \frac{U_o}{U_j}\right), \text{ dB} \quad (1)$$

The empirical parameter $k < \theta >$ is a function of the flap setting and the directivity angle. Values for this parameter, as previously stated, are determined from the product of (a)(b) given in Table 1.

In order to obtain preliminary estimates of aircraft motion effects on the flap noise, the effect of relative motion of the noise source with respect to the observer must be added to the jet relative velocity effects measured in a free jet or wind tunnel. Reference 10 gives the relative motion effects for a point dipole noise source. If it is assumed, as a rough approximation, that the flap noise field can be treated as if it were radiating from a point dipole on the trailing flap, then the dynamic effect or convective (Doppler) amplification is given by

$$\Delta(\mathrm{OASPL})_D = -40 \log \left[1 - \left(\frac{U_o}{C_o}\right) \cos \theta\right], \text{ dB} \quad (2)$$

which is an approximation even in the case of a point dipole. The Doppler effect on frequency is given by

$$f_D = \frac{f}{1 - \left(\frac{U_o}{C_o}\right) \cos \theta} \quad (3)$$

The two effects of aircraft motion can be combined into a single expression to represent the net effect on flap noise (ref. 6). Thus, the OASPL for an EBF system is given by

$$\mathrm{OASPL}_{FV} = \mathrm{OASPL}_\theta - 40 \log \left[1 - \left(\frac{U_o}{C_o}\right) \cos \theta\right] + 10\, k < \theta > \log \left(1 - \frac{U_o}{U_j}\right), \text{ dB} \quad (4)$$

and the frequency shift is given by equation (3).

Simple illustrations of the expected effect of aircraft motion on the flap noise level are shown in figure 19. In this figure, polar plots of the measured OASPL obtained in the free jet are shown by the circle symbols for the conical nozzle-wing configuration with flap settings of 10° - 20° (fig. 19(a)) and 30° - 60° (fig. 19(b)). The data are for a jet exhaust velocity of 290 m/sec and a forward speed of 53 m/sec. The inclusion of the effects of relative motion of the source with respect to the observer is shown by the solid curves in figure 19. For comparison, the data with zero airspeed (square symbols) are also included. With the source motion effect, the noise levels are increased in the forward quadrant, resulting in less attenuation than that due to the relative velocity effect measured in a free jet or wind tunnel. In the rearward quadrant, the effect of source motion decreases the noise levels resulting in additional attenuation compared with the noise levels obtained with only the relative velocity effect measured in a free jet or wind tunnel. The source motion effect is seen to increase as the directivity angles approach the nozzle axis. No effect of source motion occurs at $\theta = 90^\circ$, as is apparent from equation (2).

Further experiments are needed to determine the sensitivity of $k < \theta >$ to EBF configuration differences and ultimately these preliminary trends will have to be verified by noise measurements made during an actual aircraft flyover.

Summary of Results

The results of an investigation of the effect of relative velocity using a free jet to simulate forward velocity on the noise characteristics of model EBF powered-lift systems can be summarized as follows:

1. Airspeed attenuates the noise generated by an externally blown flap (EBF) system. The degree of attenuation depends on flap settings. A system with a highly deflected flap setting (landing) has less attenuation than one with less deflection (takeoff).

2. Noise radiation patterns were substantially unchanged over the range of conditions investigated when the model was subjected to forward velocity.

3. Overall sound pressure levels as a function of relative velocity depended on flap setting and directivity angle.

Preliminary consideration of source motion effects indicated increases in the noise above levels measured with a model in a free jet (or wind tunnel) in the forward quadrant and additional attenuation in the rearward quadrant.

Nomenclature

a,b	exponents used in Table 1
C_o	ambient speed of sound
D	nozzle diameter
D_e	equivalent nozzle diameter
f	1/3 octave band center frequency
$k < \theta >$	empirical parameter characterizing directivity angle and interaction noise effects
OASPL	overall sound pressure level, dB, re 2×10^{-5} N/M^2
SPL	1/3 octave band sound pressure level, dB, re 2×10^{-5} N/m^2
U_j	jet velocity at nozzle exhaust plane
U_o	forward velocity
θ	directivity angle measured from inlet

Subscripts

D	Doppler
FV	forward velocity
RV	relative velocity
θ	angular location

References

1. Dorsch, R. G., Kreim, W. J., Olsen, W. A., "Externally-Blown-Flap Noise," AIAA Paper 72-129, San Diego, Calif., 1972.

2. Olsen, W. A., Dorsch, R. G. and Miles, J. D., "Noise Produced by a Small-Scale, Externally Blown Flap," TN D-6636, 1972, NASA.

3. Dorsch, R. G., Goodykoontz, J. H. and Sargent, N. B., "Effect of Configuration Variation on Externally Blown Flap Noise," AIAA Paper 74-190, Washington, D.C., 1974.

4. Goodykoontz, J. H., Wagner, J. M. and Sargent, N. B., "Noise Measurements for Various Configurations of a Model of a Mixer-Nozzle Externally Blown Flap System," TM X-2776, 1973, NASA.

5. Goodykoontz, J. H., Dorsch, R. G. and Wagner, J. M., "Acoustic Characteristics of Externally Blown Flap Systems with Mixer Nozzles," AIAA Paper 74-192, Washington, D.C., 1974.

6. Dorsch, R. G., "Externally Blown Flap Noise Research," SAE Paper 740468, Dallas, Tex., 1974.

7. von Glahn, U., Groesbeck, D. and Goodykoontz, J., "Velocity Decay and Acoustic Characteristics of Various Nozzle Geometries with Forward Velocity," AIAA Paper 73-629, Palm Springs, Calif., 1973.

8. Falarski, M. D., Aiken, T. N., Aoyagi, K. and Koenig, D. G., "Comparison of the Acoustic Characteristics of Large-Scale Models of Several Propulsive-Lift Concepts," AIAA Paper 74-1094, San Diego, Calif., 1974.

9. von Glahn, U., Goodykoontz, J. and Wagner, J., "Nozzle Geometry and Forward Velocity Effects on Noise for CTOL Engine-Over-the-Wing Concept," presented at the Eighty-Sixth Meeting of the Acoustical Society of America, Los Angeles, Calif., Oct. 30 - Nov. 2, 1973, NASA TM X-71453, 1973.

10. Lighthill, M. J., "Sound Generated Aerodynamically," Proc. Roy. Soc. (London), Vol. 267A, No. 1329, May 8, 1962, pp. 147-182.

Table 1. - Relation between OASPL and relative velocity parameter, $OASPL \sim \left[U_j\ 1 - \left(\frac{U_o}{U_j}\right)^a\right]^b$, nominal values.

Configuration	Angle from nozzle inlet, θ, deg	Exponent	
		a	b
Conical nozzle			
10° - 20° flaps	40	0.6	6.5
	60	↓	↓
	80	↓	↓
	90	↓	↓
	100	.5	7
	120	↓	7
	140	↓	8
30° - 60° flaps	40	.3	6.5
	60	.25	↓
	80	.2	↓
	90	.3	7
	100	.3	8
Mixer nozzle			
10° - 20° flaps	40	.6	7
	60	.7	↓
	80	↓	↓
	90	↓	↓
	100	↓	↓
	120	↓	↓
	140	.8	8
30° - 60° flaps	40	.1	7
	60	.1	↓
	80	.2	↓
	90	.3	↓
	100	.4	8

Table 2. - Low Frequency Noise Source Characteristics; $SPL \sim (U_j - U_o)^{k<\theta>}$

Flap deflection angle, deg	Nozzle type	Jet relative velocity exponent, $k<\theta>$		Directivity angle of peak SPL, deg	
		static	with airspeed	static	with airspeed
10 - 20	Conical	3.2	8.0	90	100
30 - 60	Conical	3.5	4.0	< 60	< 60
10 - 20	Mixer	4.8	11.0	> 0	60
30 - 60	Mixer	7.0	7.0	< 60	< 60

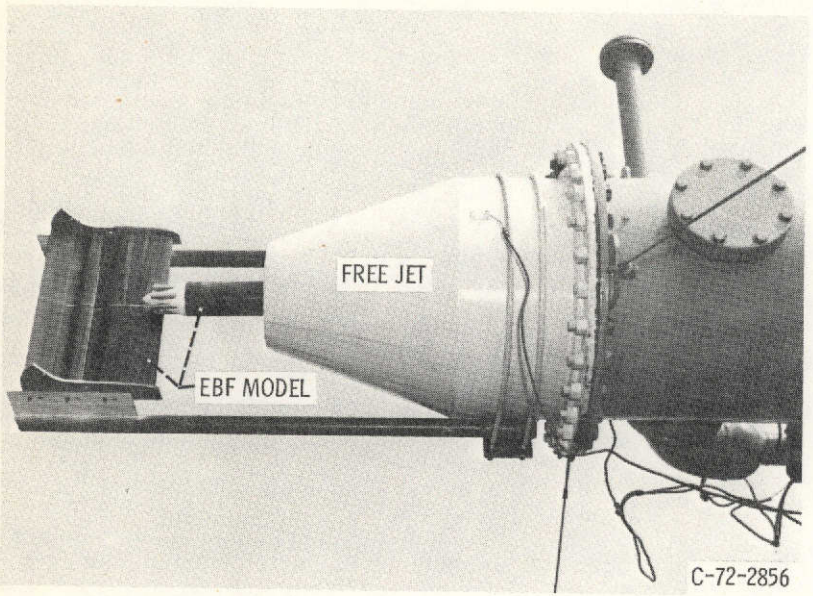

Figure 1. - Externally blown flap airspeed-effect test installation with 8-tube mixer nozzle.

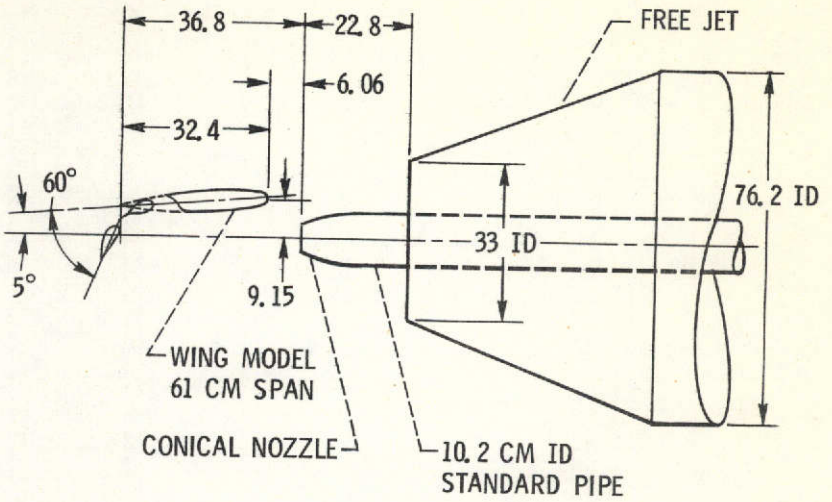

(a) GENERAL LAYOUT.

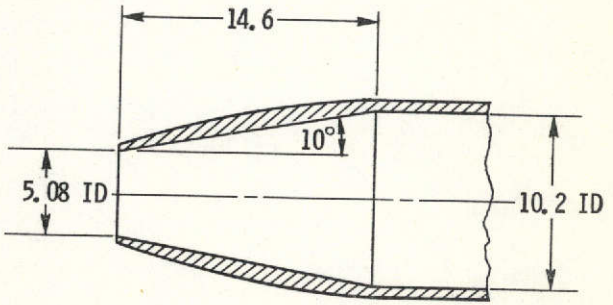

(b) CONICAL NOZZLE DETAIL.

Figure 2. - Conical nozzle - wing installation in free jet. Wing flaps in landing position, 30°-60°. (All dimensions in centimeters.)

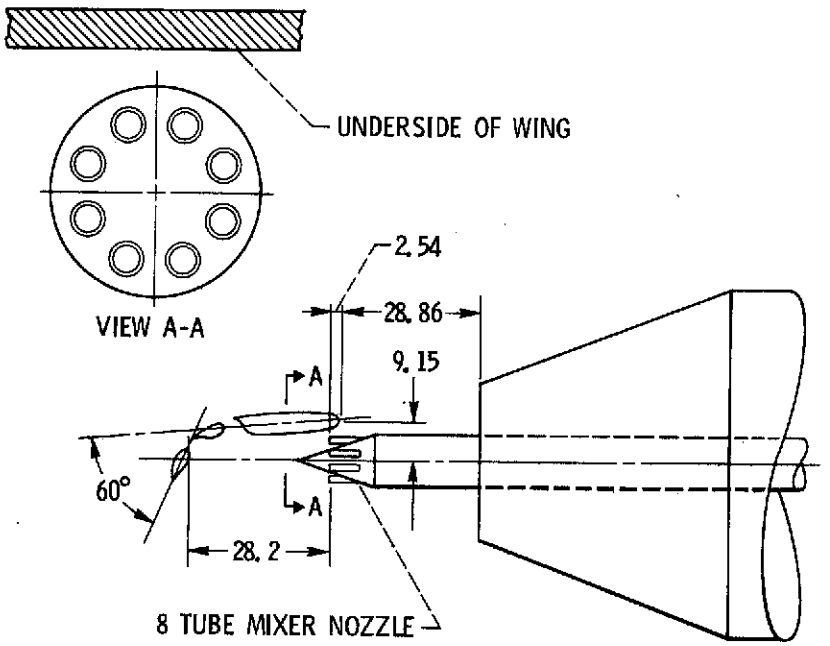

(a) GENERAL LAYOUT.

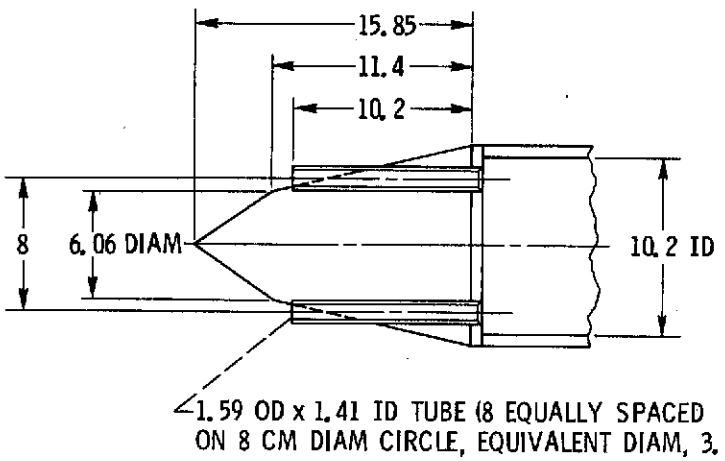

(b) 8 TUBE MIXER NOZZLE DETAIL.

Figure 3. - 8 Tube mixer nozzle - wing installation in free jet. Wing flaps in landing position, 30°-60°. (All dimension in centimeters).

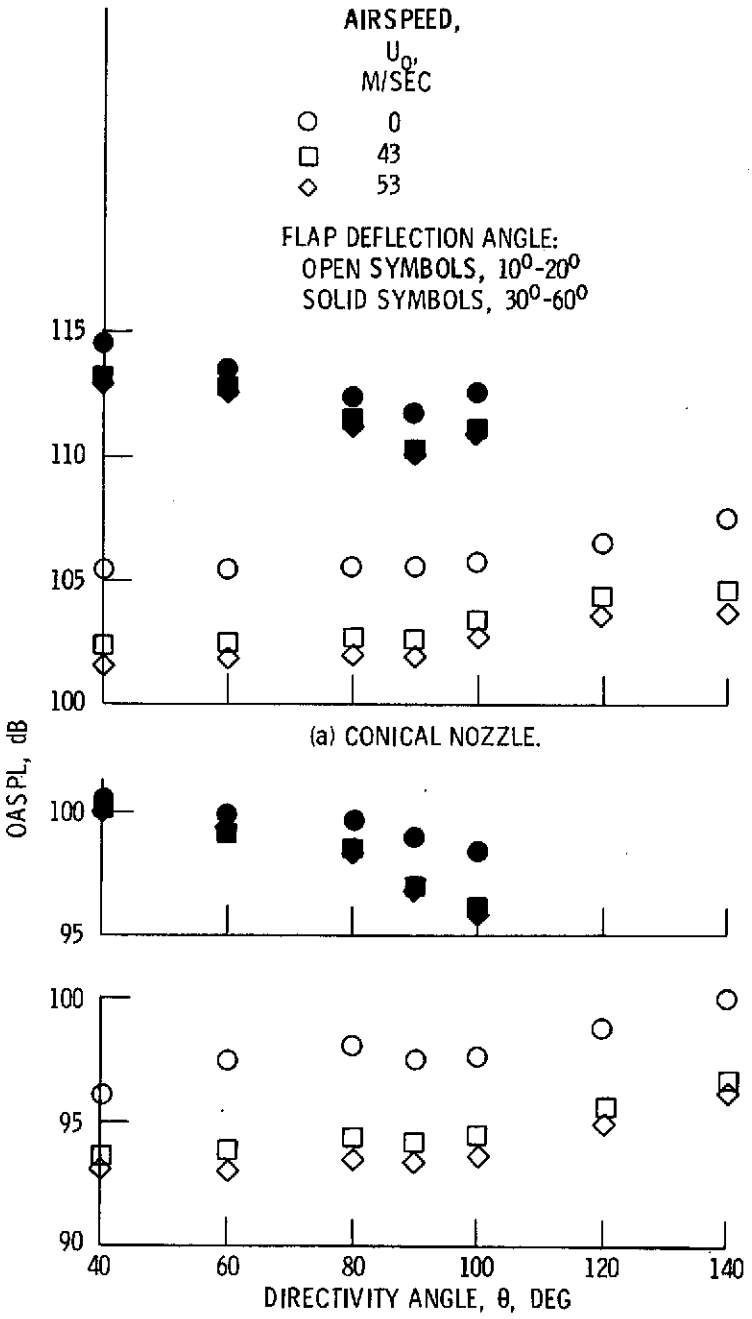

Figure 4. - Variation of OASPL with directivity angle. U_j, 290 m/sec.

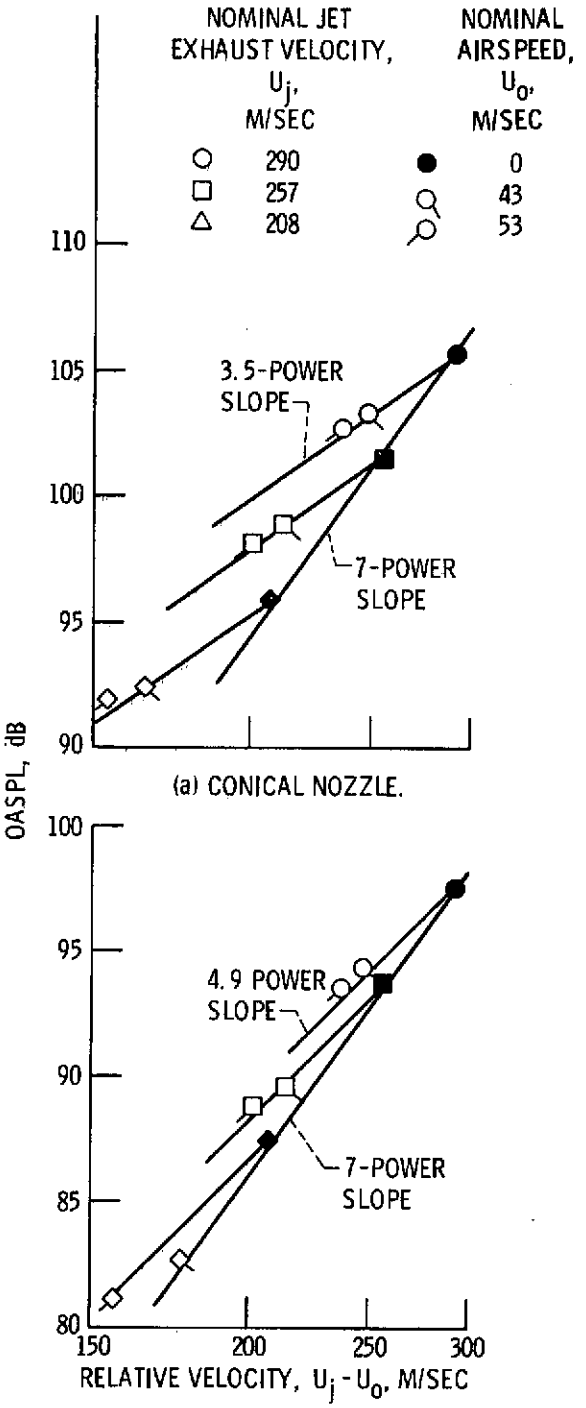

Figure 5. - Variation of OASPL with relative velocity. Flap deflection angle, 10^0-20^0; directivity angle, 100^0.

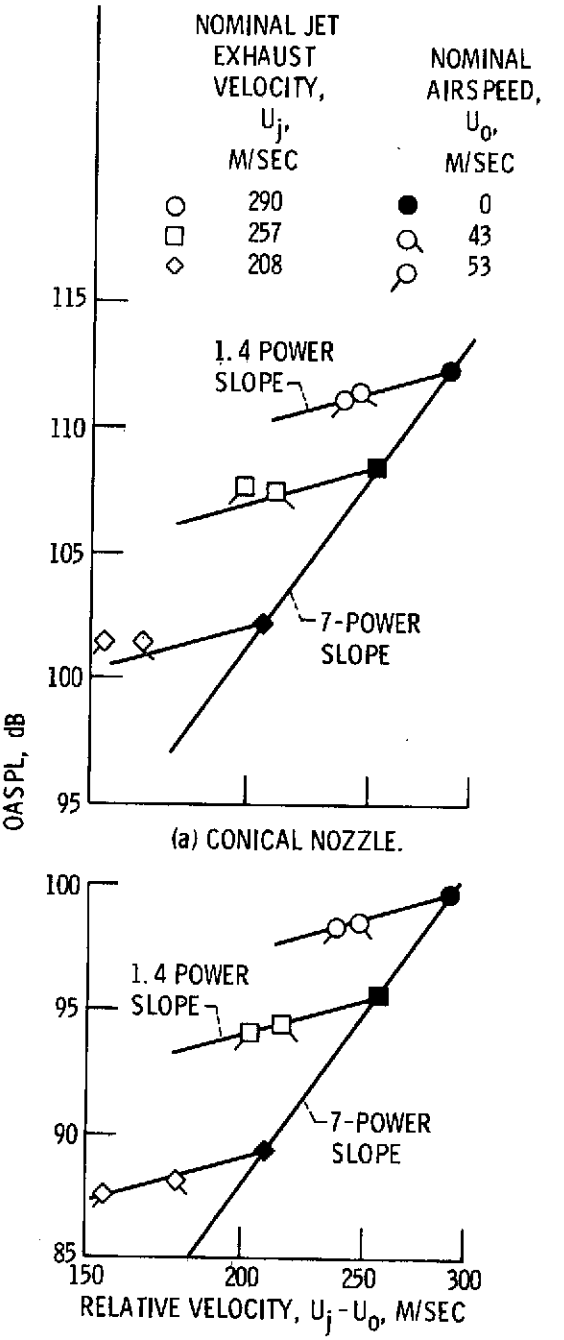

Figure 6. - Variation of OASPL with relative velocity. Flap deflection angle, 30^0-60^0; directivity angle, 80^0.

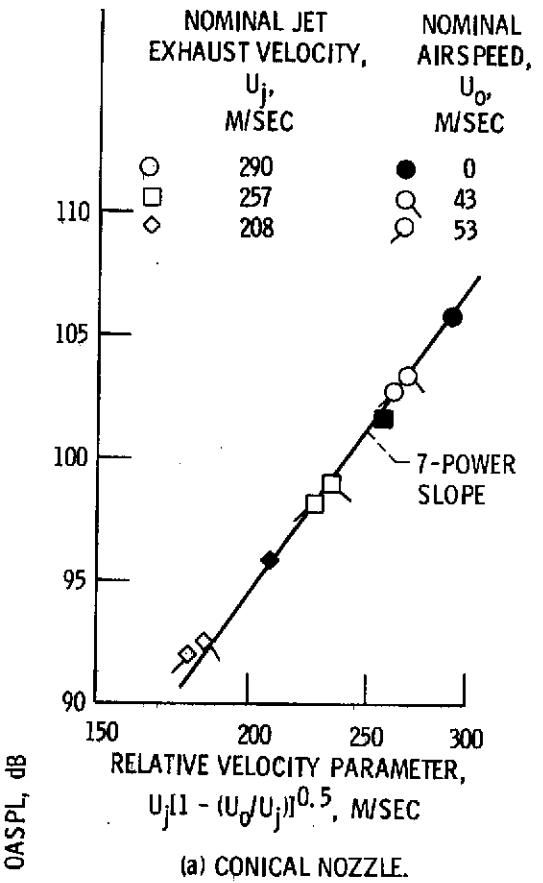

(a) CONICAL NOZZLE.

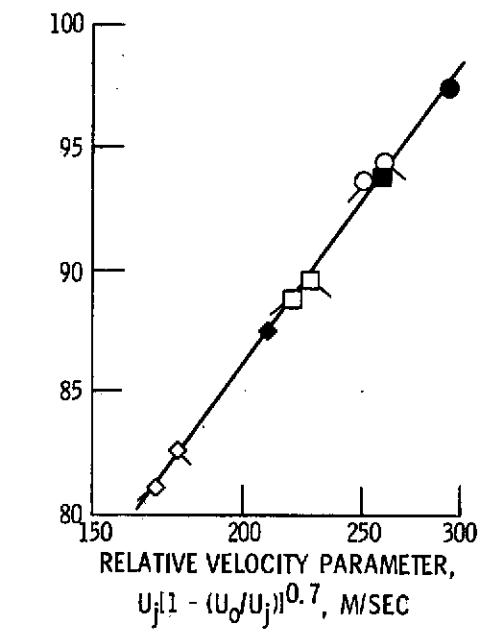

(b) MIXER NOZZLE.

Figure 7. - Correlation of OASPL with relative velocity parameter. Flap deflection angle, 10^0-20^0; directivity angle, 100^0.

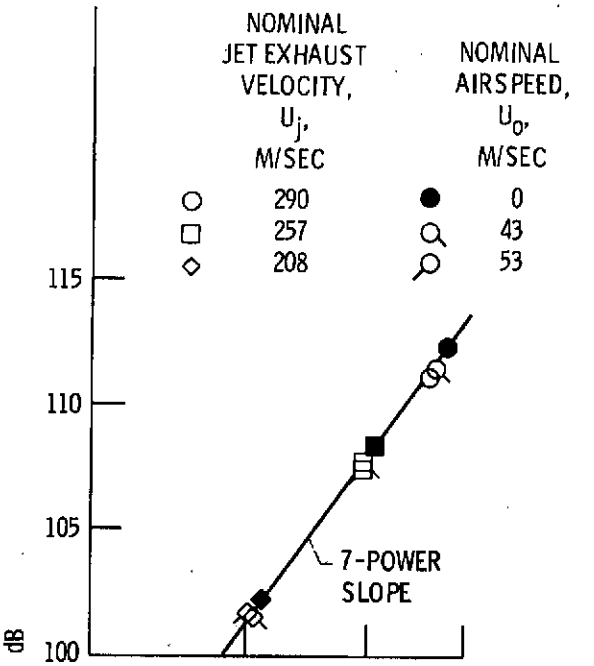

(a) CONICAL NOZZLE.

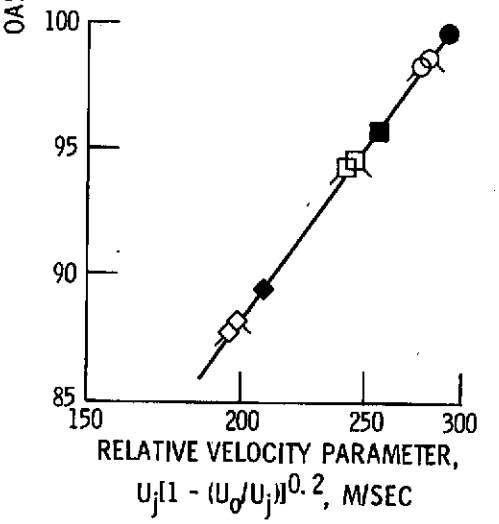

(b) MIXER NOZZLE.

Figure 8. - Correlation of OASPL with relative velocity parameter. Flap deflection angle, 30^0-60^0; directivity angle, 80^0.

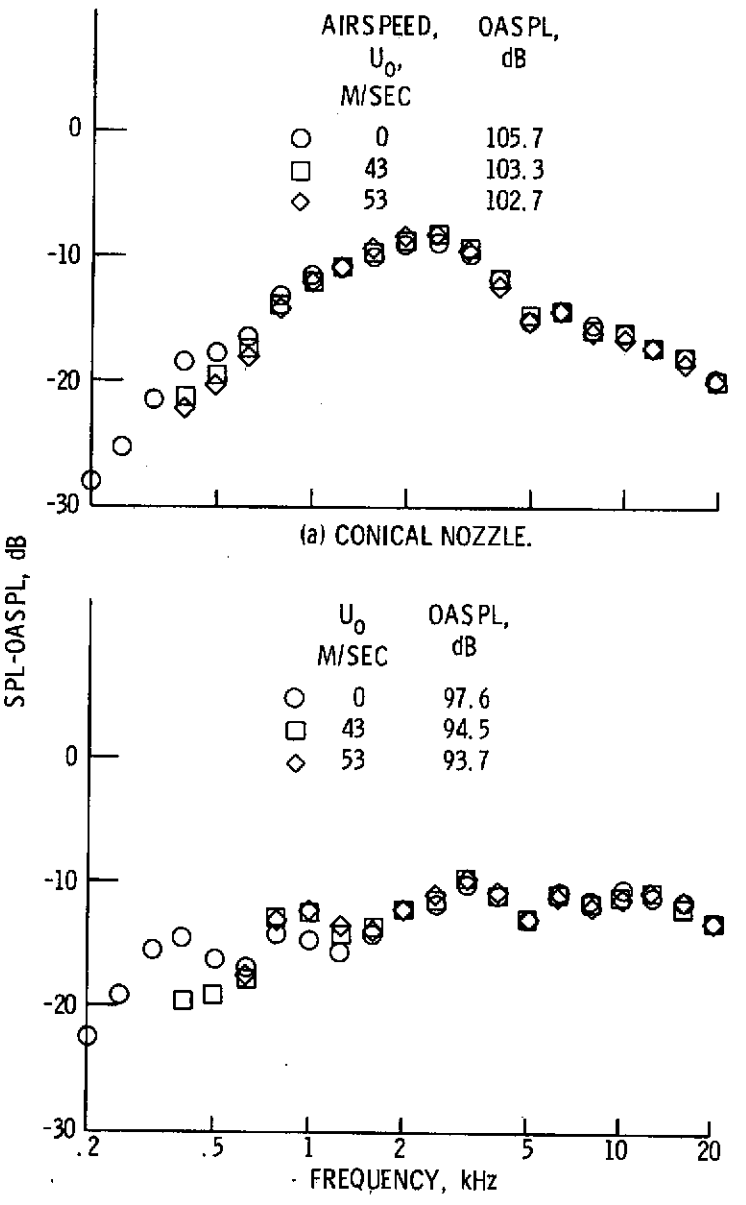

Figure 9. - Normalized spectra with flap deflection angle of 10^0-20^0 as a function of frequency. Directivity angle, 100^0; U_j, 290 m/sec.

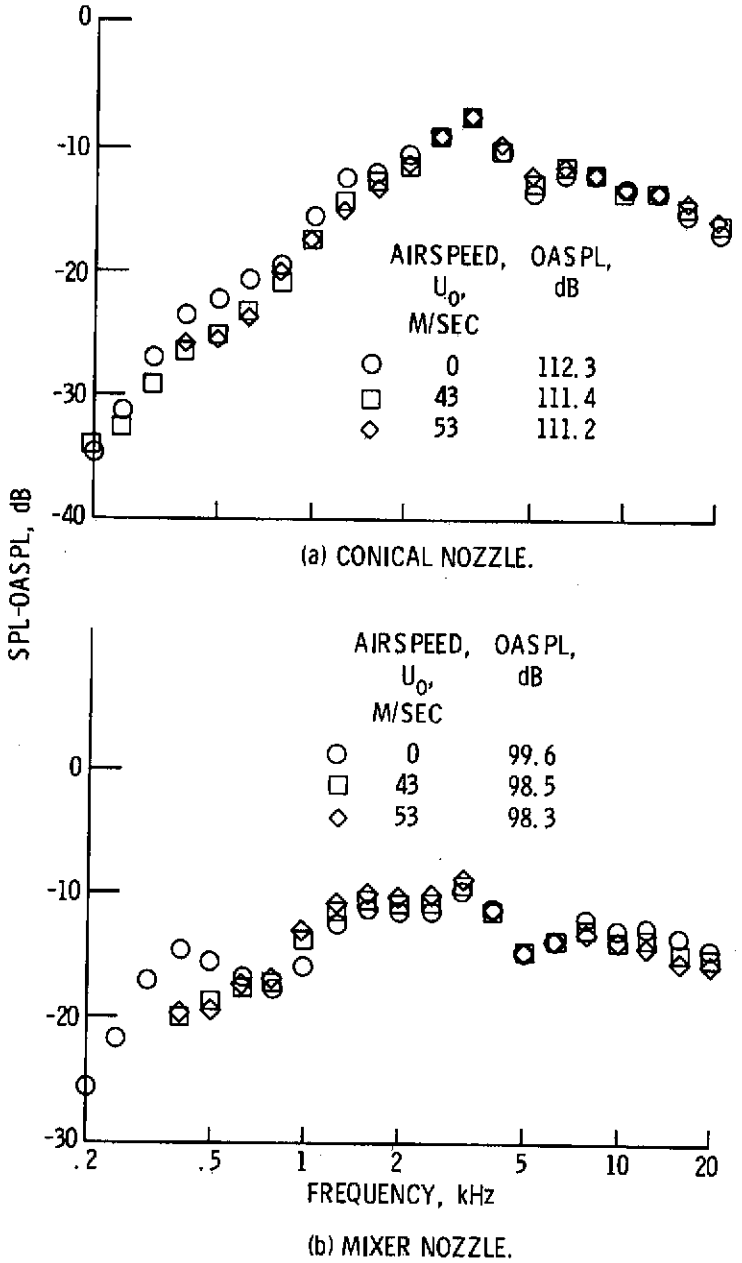

Figure 10. - Normalized spectra with flap deflection of 30^0-60^0 as a function of frequency. Directivity angle, 80^0; U_j, 290 m/sec.

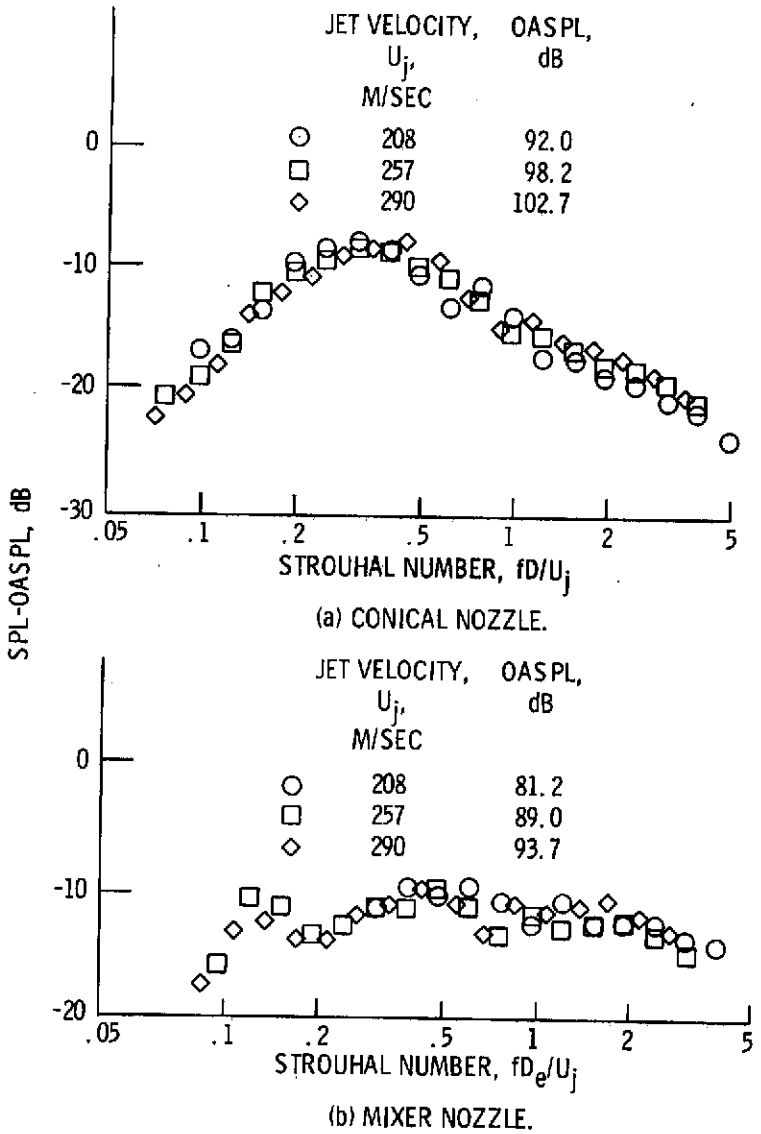

Figure 11. - Normalized spectra as a function of Strouhal number for flap deflection angle of 10^0-20^0. Directivity angle, 100^0; U_0, 53 m/sec.

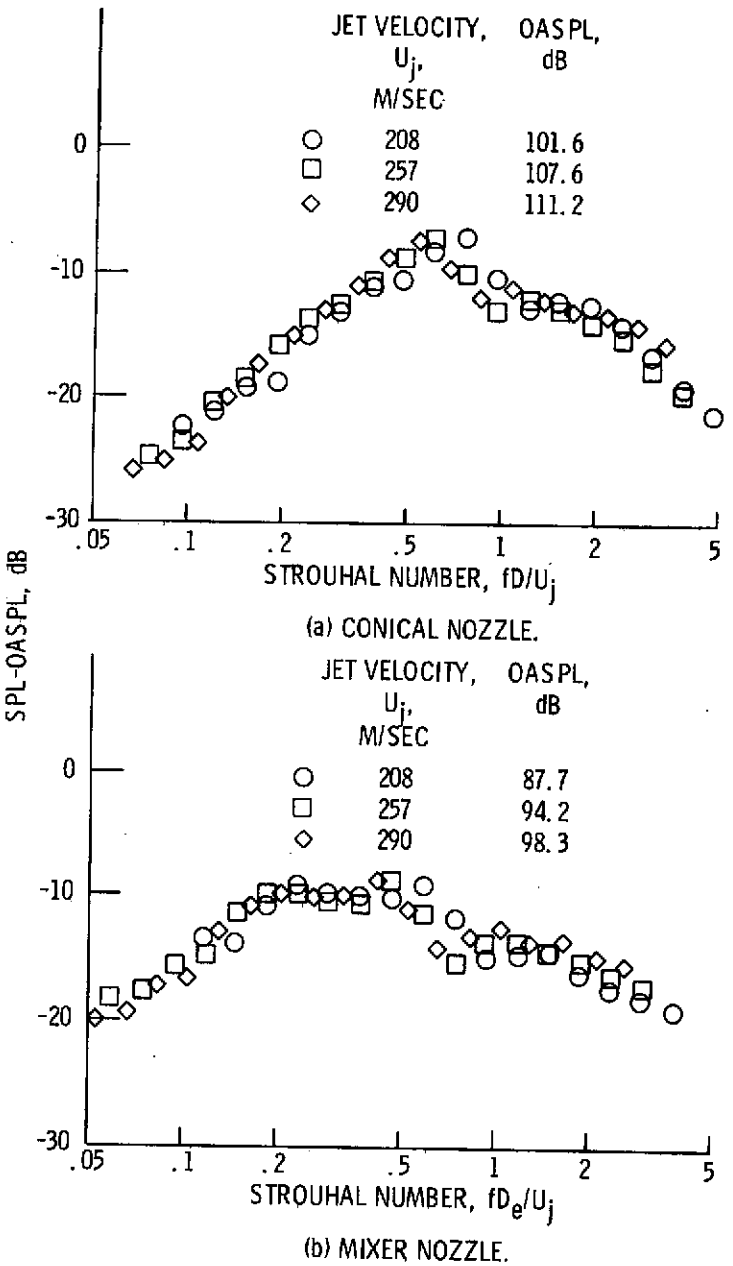

Figure 12. - Normalized spectra as a function of Strouhal number for flap deflection angle of 30^0-60^0. Directivity angle, 80^0; U_0, 53 m/sec.

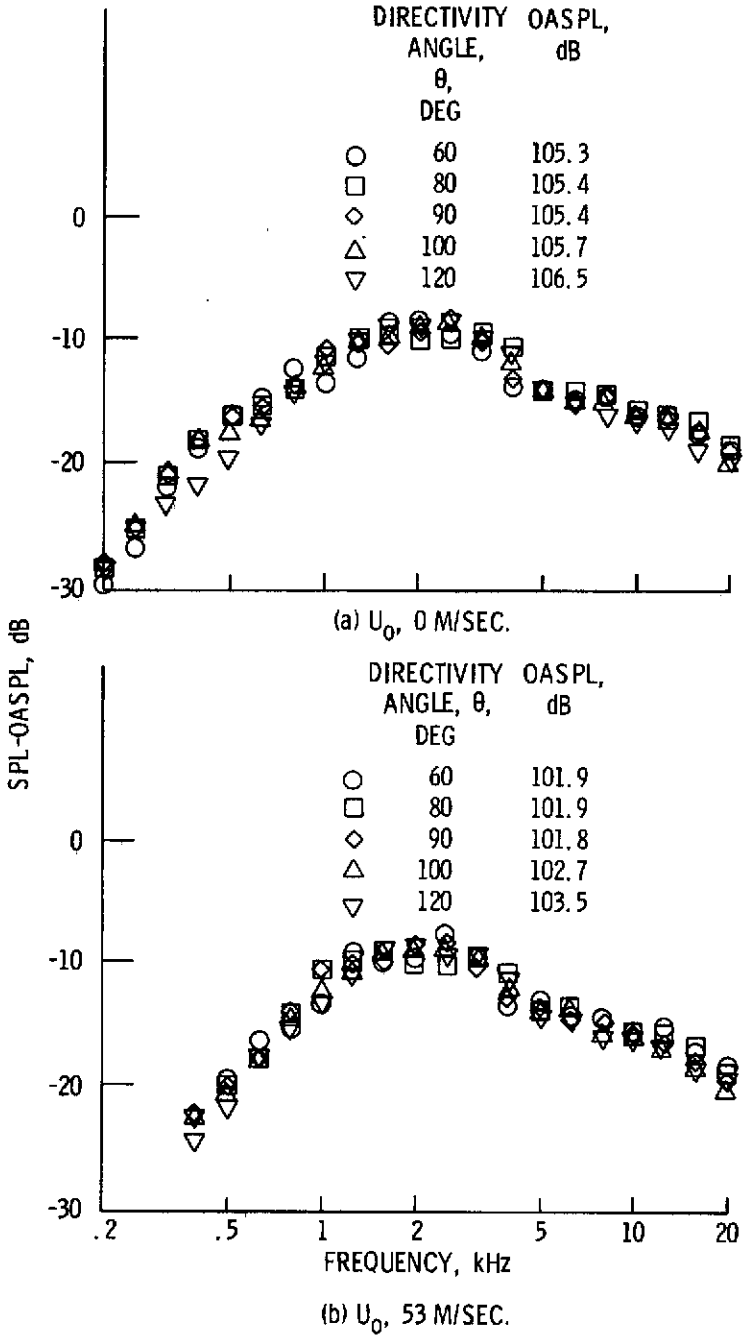

Figure 13. - Normalized spectra with conical nozzle as a function of frequency for various directivity angles. Flap deflection angle, 10^0-20^0; U_j, 290 m/sec.

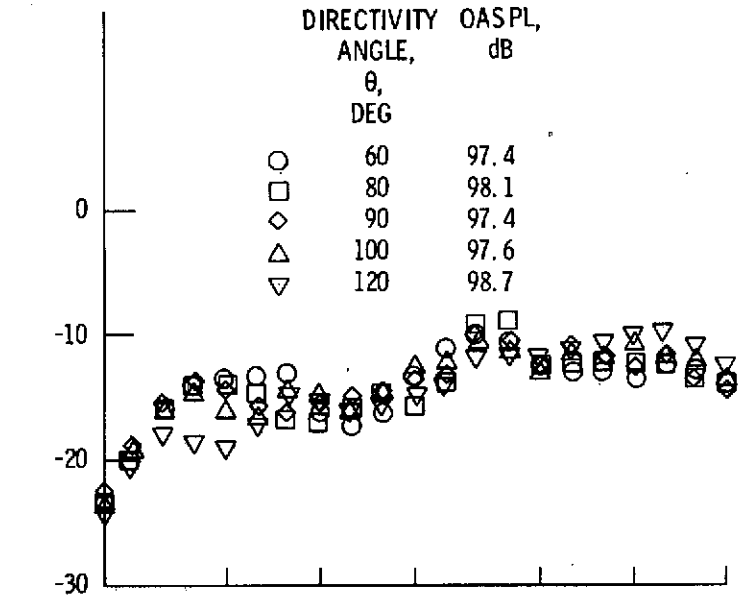

(a) U_0, 0 M/SEC.

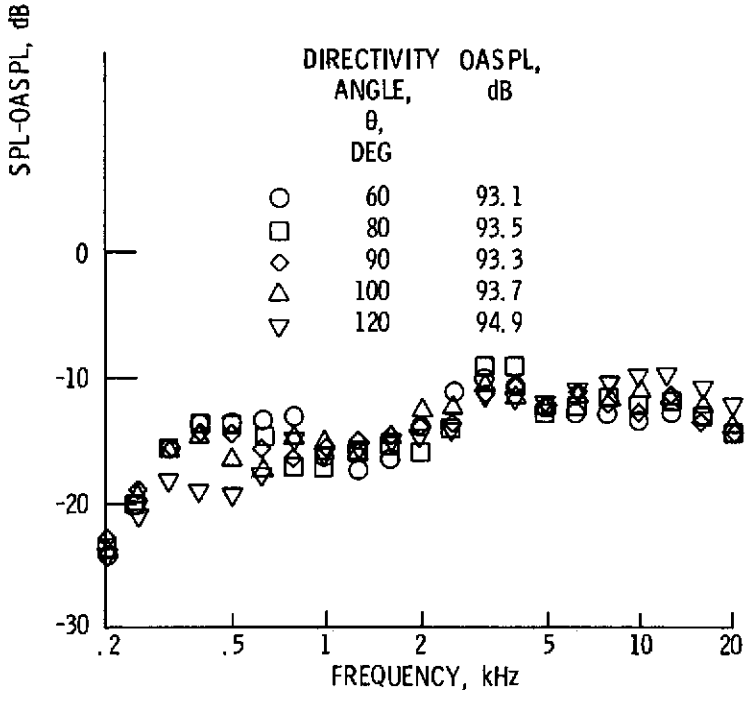

(b) U_0, 53 M/SEC.

Figure 14. - Normalized spectra with mixer nozzle as a function of frequency for various directivity angles. Flap deflection angle, 10^0-20^0; U_j, 290 m/sec.

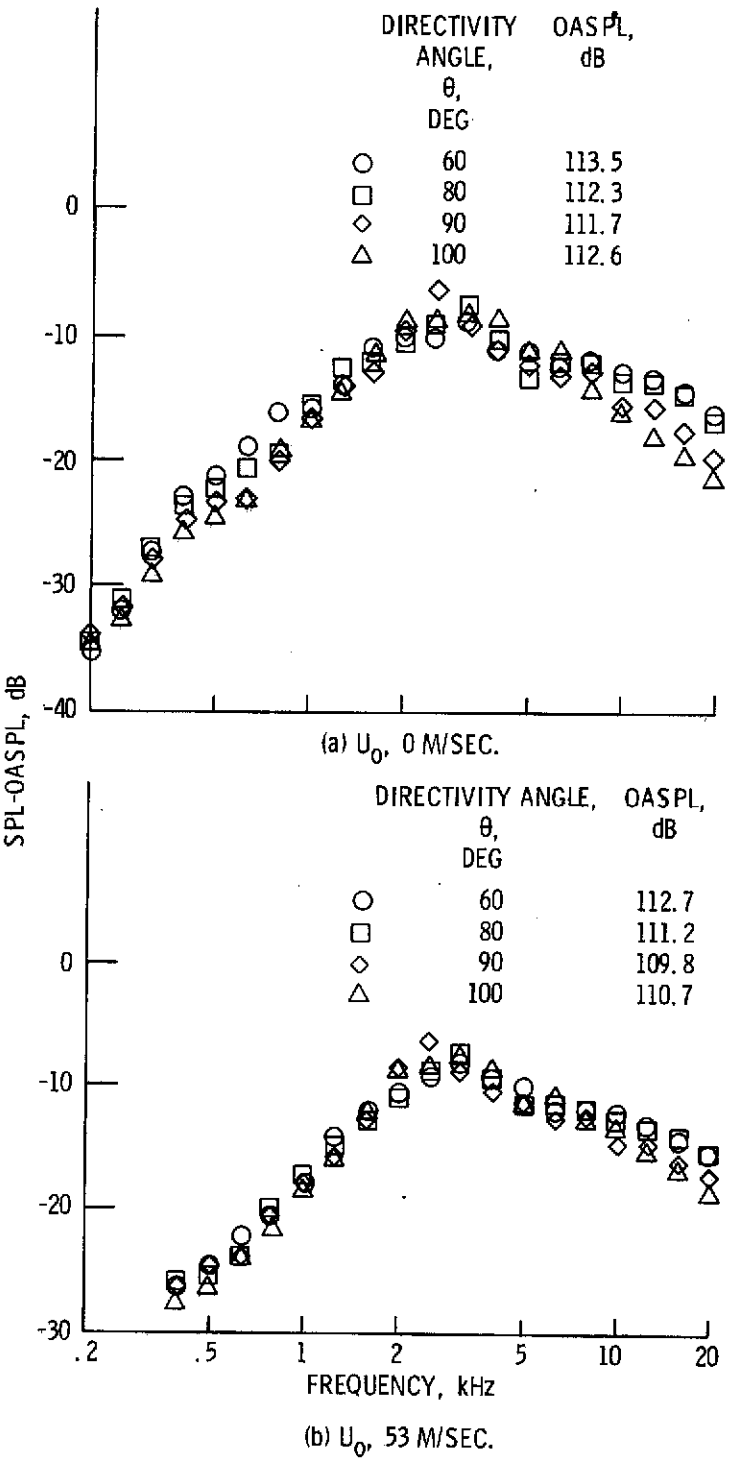

Figure 15. - Normalized spectra with conical nozzle as a function of frequency for various directivity angles. Flap deflection angle, 30^0-60^0; U_j, 290 m/sec.

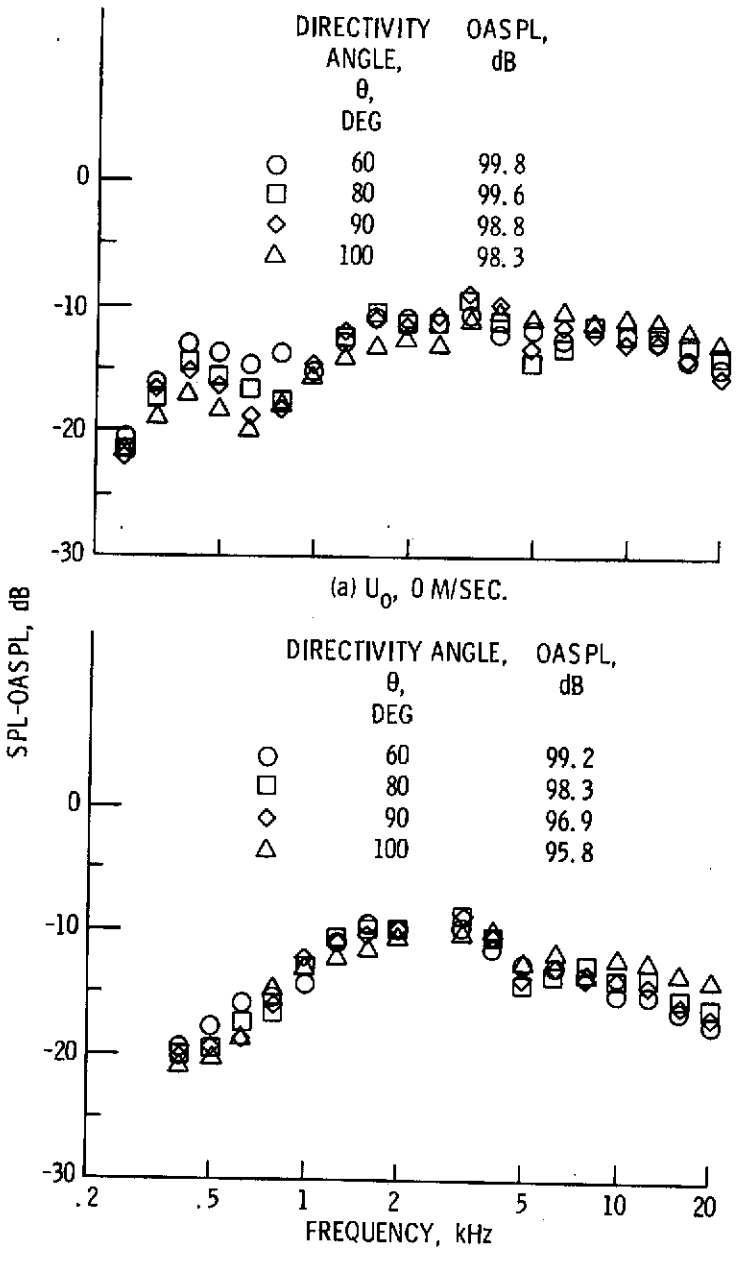

Figure 16. - Normalized spectra with mixer nozzle as a function of frequency for various directivity angles. Flap deflection angle, 30^0-60^0; U_j; 290 m/sec.

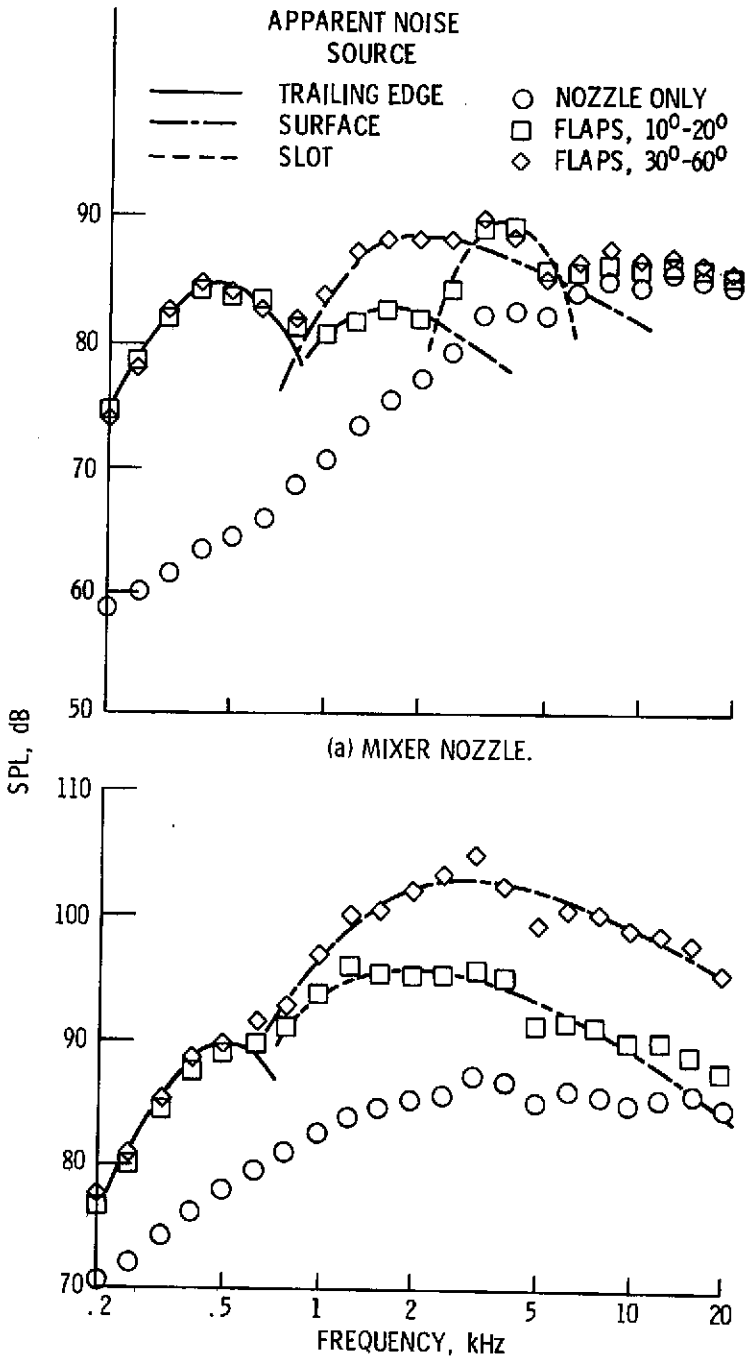

Figure 17. - Jet-flap interaction noise spectra as a function of frequency for static conditions. U_j, 290 m/sec; directivity angle, 80°.

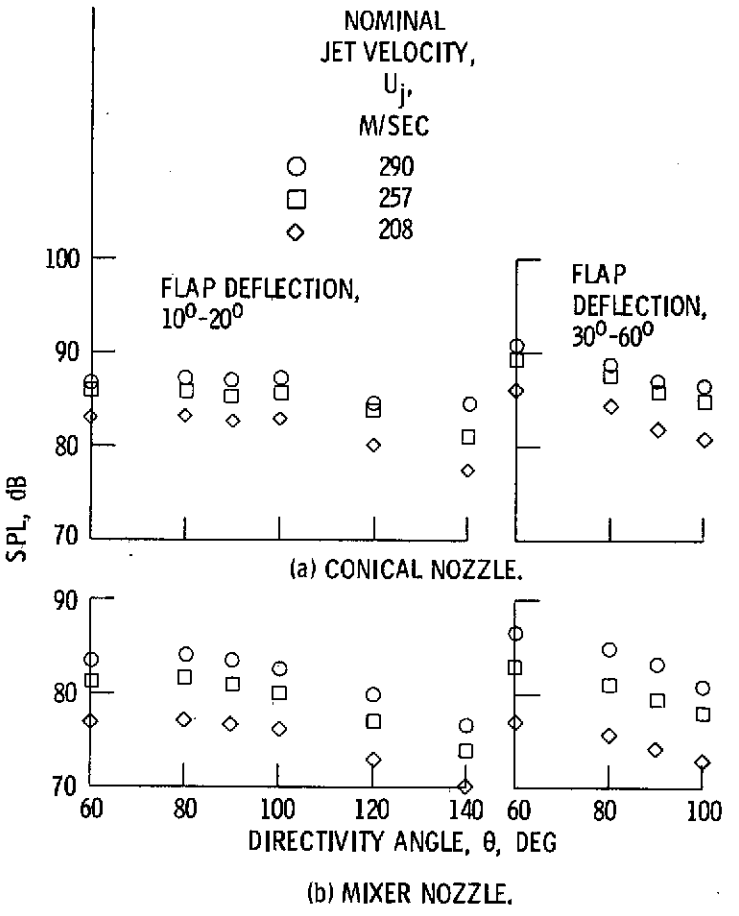

Figure 18. - Peak trailing edge interaction noise SPL at 500 Hz as a function of directivity angle for static conditions.

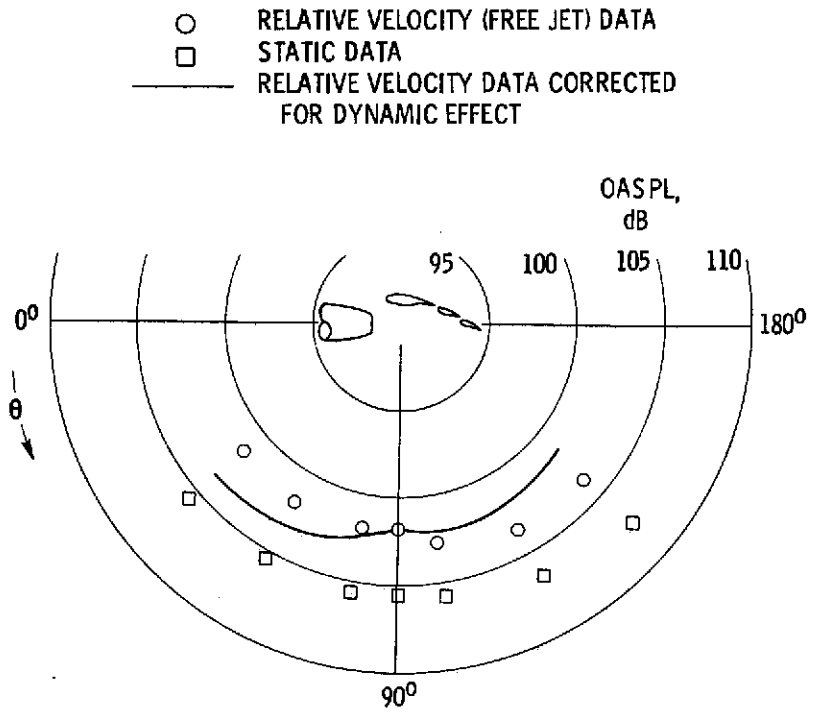

(a) FLAP DEFLECTION, 10°-20°.

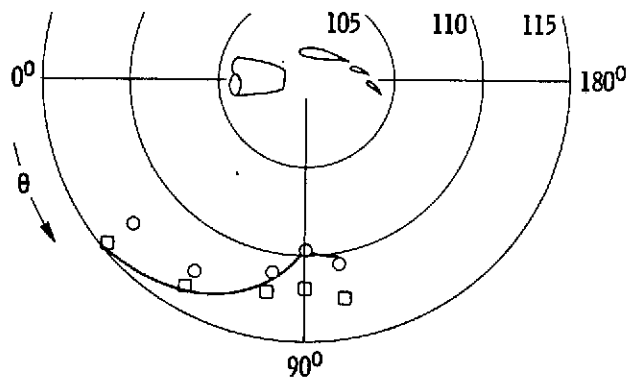

(b) FLAP DEFLECTION, 30°-60°.

Figure 19. - Typical effect of aircraft motion on flap noise level measured in free jet. U_j, 290 m/sec; U_o, 53 m/sec; conical nozzle.